


Insight into RNA–DNA primer length counting by human primosome

Andrey G. Baranovskiy, Alisa E. Lisova, Lucia M. Morstadt, Nigar D. Babayeva and Tahir H. Tahirov ^{*}

Eppley Institute for Research in Cancer and Allied Diseases, Fred & Pamela Buffett Cancer Center. University of Nebraska Medical Center, Omaha, NE, USA

Received April 21, 2022; Revised May 19, 2022; Editorial Decision May 20, 2022; Accepted June 08, 2022

ABSTRACT

The human primosome, a four-subunit complex of primase and DNA polymerase alpha (Pol α), synthesizes chimeric RNA–DNA primers of a limited length for DNA polymerases delta and epsilon to initiate DNA replication on both chromosome strands. Despite recent structural insights into the action of its two catalytic centers, the mechanism of DNA synthesis termination is still unclear. Here we report results of functional and structural studies revealing how the human primosome counts RNA–DNA primer length and timely terminates DNA elongation. Using a single-turnover primer extension assay, we defined two factors that determine a mature primer length (~35-mer): (i) a tight interaction of the C-terminal domain of the DNA primase large subunit (p58_C) with the primer 5'-end, and (ii) flexible tethering of p58_C and the DNA polymerase alpha catalytic core domain (p180_{core}) to the primosome platform domain by extended linkers. The obtained data allow us to conclude that p58_C is a key regulator of all steps of RNA–DNA primer synthesis. The above-described findings provide a notable insight into the mechanism of DNA synthesis termination by a eukaryotic primosome, an important process for ensuring successful primer handover to replication DNA polymerases and for maintaining genome integrity.

INTRODUCTION

Human primosome is a multifunctional complex with a key role in DNA replication (1,2). It is also implicated in a variety of other cellular processes, including telomere maintenance (3,4), innate immunity (5–7) and genome stability (8–10), and it is an emerging candidate for anticancer therapy (11). Primosome is the essential enzyme producing RNA–DNA chimeric primers for the replication of both leading and lagging strands after recruiting either DNA

polymerase epsilon (Pol ϵ) or delta (Pol δ) (12,13). The human primosome comprises the two-subunit primase, with catalytic (p49) and regulatory (p58) subunits, and the two-subunit DNA polymerase α (Pol α), with catalytic (p180) and accessory (p70) subunits (1). p180 contains a catalytic core (p180_{core}) and a C-terminal domain (p180_C), while p58 has N-terminal (p58_N) and C-terminal (p58_C) domains. Primosome forms an elongated platform p49–p58_N–p180_C–p70, which holds p58_C and p180_{core} either stationary or flexibly by linkers p58_N–p58_C (L1, residues 253–270) and p180_{core}–p180_C (L2, residues 1250–1267) (6,14–16) (Figure 1).

The primase is responsible for the initiation, elongation, and termination of RNA primer synthesis when its length reaches nine nucleotides (nt) (15,17–19), and then for its intramolecular transfer to the catalytic subunit of Pol α (1,20). After receiving the RNA primer, Pol α extends it to a limited degree (21) using deoxyribonucleotide-triphosphates (dNTPs). The concerted RNA–DNA primer synthesis by the two catalytic centers of primosome is tightly regulated; Pol α is inactive while primase works, and *vice versa* (15,20). Previously we explored the structural basis for such regulation, including the initiation, elongation, and termination steps of RNA primer synthesis by primase and the following primer transfer to Pol α (15). Despite this breakthrough, the factors that regulate the subsequent steps resulting in generation of an RNA–DNA primer of defined length are unknown.

In this work, we conducted a series of biochemical experiments along with structure-based modeling studies to gain insight into the intrinsic mechanism of DNA synthesis elongation and termination by eukaryotic primosome.

MATERIALS AND METHODS

Protein expression and purification

Expression and purification to homogeneity of the human primase heterodimer and its mutants (14,22), human primosome (p49–p58–p180–p70) (23), and the Pol α catalytic core (23) have been described elsewhere. As previously re-

^{*}To whom correspondence should be addressed. Tel: +1 402 559 7608; Fax: +1 402 559 3739; Email: ttahirov@unmc.edu

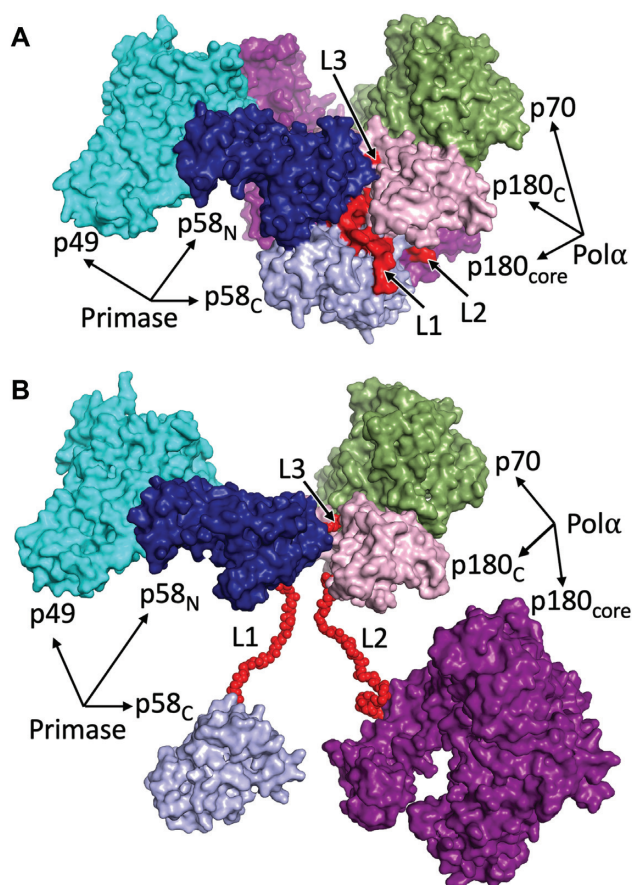


Figure 1. Architecture of human primosome. The platform (p49–p58_N–p180_C–p70) can hold p58_C and p180_{core} either stationary, as in apo-form (A) or flexibly by linkers (B). The figures were produced using crystal structure of primosome apo-form (PDB accession code 5exr). In panel B the positions of p58_C and p180_{core} were moved to arbitrary positions. The linkers L1 and L2 were modeled to show their relative locations. Additional flexibility to platform is provided by linker L3.

ported, the N-terminus of p180 (residues 1–334) has been deleted because it is poorly folded (4) and is not required for activity and interaction with other subunits (15). In the deletion mutants $\Delta 5$, $\Delta 10$, $\Delta 15$, and $\Delta p58_C$, the following regions were removed in p58: 256–260, 256–265, 256–270 and 266–560, respectively. In the mutant Ins5, residues GSASG were added after Ser263 of p58. Pol $\alpha\Delta 8$ with a deleted region 1254–1261 was generated in this work by the site mutagenesis protocol according to (24).

Oligonucleotides for functional studies

Sequences of all oligonucleotides are provided in Table 1. Oligonucleotides without 5'-triphosphate were obtained from IDT, Inc. The 5-mer RNA primer P5 containing the 5'-triphosphate (5'-pppGGCGG) was obtained as described previously using DNA duplex T8:P4 and the RNA polymerase of bacteriophage T7 (25). Template:primers containing a chimeric RNA–DNA primer P2 were obtained by ligation using the corresponding template, the primers P5 and P6 (Supplemental Figure S1), and RNA ligase 2 of bacteriophage T4 (New England BioLabs, Inc.). Reactions

were incubated for one hour at 25°C and ligated duplexes were purified by 1ml monoQ column (Cytiva) at 50°C.

Primer extension assay

DNA-synthetic activity was tested in 10 μ l reaction containing 0.6 μ M template:primer, 0.2 μ M enzyme, 10 μ M dNTPs, 0.1 μ M [α -³²P]-dCTP (3000 Ci/mmol; PerkinElmer, Inc.), 10 μ M trap, and the buffer: 30 mM Tris–HEPES, pH 7.8, 120 mM KCl, 30 mM NaCl, 1% glycerol, 2 mM TCEP, 5 mM MgCl₂ and 0.2 mg/ml BSA. The trap was a T6:P3 duplex containing the dideoxy-cytosine at the primer 3'-end to make a dead-end complex with Pol α . All primosome mutants were prepared in the reaction buffer by mixing 1 μ M Pol α or Pol $\alpha\Delta 8$ with a corresponding primase mutant added at 20% molar excess (Supplemental Figure S2). The enzyme was pre-incubated with a template:primer in 5 μ l for 1 min on ice and for 10 s at 35°C, then reaction was initiated by addition of 5 μ l solution containing dNTPs and trap. Reactions were incubated in PCR tubes on a water bath for 30 s at 35°C and stopped by mixing with equal volume of formamide loading buffer (90% v/v formamide, 50 mM EDTA, pH 8, 0.02% Bromophenol blue), heated at 95°C for 1 min, and resolved by 20% urea–PAGE [UreaGel System (19:1 acrylamide/bisacrylamide), National Diagnostics] for 2.5 h at 3000 V. The reaction products were visualized by phosphorimaging (Typhoon FLA 9500, Cytiva). All activity gels were repeated at least two times.

Binding studies. Analysis of binding kinetics was done at 23 °C on Octet K2 (Sartorius AG). A template T7 with a biotin at the 5'-end annealed to the primer P2 (Table 1) was prepared by ligation and immobilized on a streptavidin-coated biosensor (SAX, Sartorius AG) at 50 nM concentration for 7 min at 500 rpm; sensors were then blocked by incubating for 2 min in 10 μ g/ml biocytin. Binding studies were conducted in a 96-well microplate (Greiner Bio-One) in buffer containing 30 mM Tris–HEPES, pH 7.8, 150 mM NaCl, 5 mM MgCl₂, 2 mM TCEP and 0.002% Tween 20. Each binding cycle starts with a baseline step by incubating a sensor for 30 s in a well with buffer. After that, the sensor moves to a well with p58_C solution to begin an association step. After sensor saturation with an analyte (p58_C), it returns to the baseline well to start a dissociation step. Approximately 20 min was required for complete dissociation of p58_C from the sensor loaded with T7:P2. All steps were conducted at shaking speed of 1000 rpm. Data Analysis HT software (version 11.1, Sartorius AG) was used to calculate binding constants (k_{on} , k_{off} and K_D) by using global fitting. The average value and standard deviation were calculated from three independent experiments.

Modeling. For the modeling of primosome elongation complexes, we used the coordinates of primosome in apo form (pdb code: 5exr) (15), p180_{core} with an RNA-primed DNA template and dCTP (4qcl) (26), p58_C with an RNA-primed DNA template (5f0q) (15), and an ideal B-DNA generated with Coot (27). Modeling was performed by constructing several template:primer duplexes up to 33-base-pair (bp) by combining the duplex parts from the crystal structures as well as ideal B-DNA in the case of duplexes

Table 1. Oligonucleotides used in this study

Name	Sequence ^a	Application	Length
T1	ACCAACACTAACAACAACATACAACATCAAGAGGTCGTGCCGCCAAAAA ^b	Primer extension	50
T2	ACCAACACTAAAAACAACAACATACAACATCAAGAGGTCGTGCCGCCAAAAA		50
T3	ACCAACTCTATCACACTTCATACCACATCAAGAGGTCGTGCCGCCAAAAA		50
T4	ACCAACTCTATCCAACCTTCATACCACATCAAGAGGTCGTGCCGCCAAAAA		50
T5	ACCAACTCTATCCTACTTCATACCACATCAAGAGGTCGTGCCGCCAAAAA		50
P1	<i>GGCGGCACGACC</i>	Trap	12
P2	<i>pppGGCGGCACGACC</i> ^c		12
T6	<u>ATAATGGCAGCTCTGGC</u>		17
P3	<i>GCCAGAGCUGC/3ddC/</i>	Binding kinetics	12
T7	<u>/5Biotin/AATACATAAGGTCGTGCCGCCAATAA</u>		26
P2	<i>pppGGCGGCACGACC</i>	P5 synthesis	12
T8	<u>CCGCCTATAGTGAGTCGTATTA</u>		22
P4	<u>AATACGACTCACTATAGG</u>		18
P5	<i>pppGGCGG</i>	P2 synthesis	5
P6	<i>pCAGACC</i>		7

^aSequences are listed in order from 5'-end to 3'-end.

^bThe regions complementary to a primer are underlined.

^cThe ribonucleotides are in italics; ppp indicates the 5'-triphosphate group.

^dddC indicates dideoxy cytosine.

over 15-bp, by manual adjustment, and by using 'regularize zone' option of Coot software (27).

RESULTS

Primosome autonomously controls the length of an RNA–DNA primer

The design of our experiments was based on the hypothesis that p58_C stays bound to the template:primer upon RNA primer transfer from p49 to Pol α and the following primer extension with dNTPs. This hypothesis is based on the high affinity of p58_C to the template:primer ($K_d = 36$ nM) (25) and its ability to share the 9-mer RNA primer with p180_{core} (1,15). We first compared primer extension by p180_{core} and primosome using a pre-annealed template:primer, which mimics the native primosome substrate (1). It presents a 50-mer DNA template annealed to a 12-mer chimeric primer (5'-pppGGCGGCACGACC, RNA region is in italics) containing nine ribonucleotides with the triphosphate group at the 5'-end and three deoxynucleoside monophosphates (dNMPs) at the 3'-end (Supplemental Figure S1). To observe the products generated during a single round of primer extension, a DNA trap (T6:P3 template:primer with the blocked 3'-end; Table 1) was added together with dNTPs at reaction start to prevent repriming events. For example, in the absence of a DNA trap, p180_{core} mainly generates a 45-mer product, which suggests multiple binding events (Figure 2A, lane 1). At single-turnover conditions (with a DNA trap), we observe the actual p180_{core} processivity (lane 2), which is significantly lower than in the absence of a trap.

A comparison of the primer extension products generated at single-turnover conditions on the templates T1 and T2 by p180_{core} (Figure 2A, lanes 2 and 3) and primosome (Figure 2B, lanes 1 and 2) revealed that primosome makes longer products, indicative of increased processivity of DNA synthesis. On the templates with a reduced AT-content, p180_{core} showed higher processivity of DNA synthesis than on T1 and T2 (Figure 2A, lanes 4–6, compared to lanes 2 and 3) resulting in generation of a notable amount of 35–41-mer products. In contrast, when the primosome performed DNA synthesis on T3–T5, the level

of primers with a length exceeding 37nt is significantly reduced (Figure 2B, lanes 3–5, compared to Figure 2A, lanes 4–6). Thus, Pol α processivity significantly depends on the template sequence, while for primosome such dependence is much weaker.

These data indicate that primosome has the ability to regulate primer elongation by Pol α and to terminate DNA synthesis, which results in generation of RNA–DNA primers with a length of 32–37nt, defined here as mature primers. Products with a similar length were obtained in the course of pulse-chase experiments conducted in the SV40 replication system (21). Our data revealed that besides Pol α there are additional factors in primosome that control the primer length. These factors increase processivity of DNA synthesis when the primer is shorter than 32-mer and gradually reduce processivity when its length exceeds 37nt.

p58_C and primosome linkers define the length of an RNA–DNA primer

To test the hypothesis that p58_C regulates the primer length by holding the primer 5'-end (25), we repeated the assay using a primosome with deleted p58_C or a template:primer without a 5'-triphosphate on the primer strand. In both cases the primosome generated shorter products (Figure 2C, lanes 1 and 2, compared to lane 1 of panel B), similar to that seen in reactions with p180_{core} (Figure 2A, lane 2). Overall, these results indicate that p58_C is associated with the primer 5'-end when p180_{core} extends the primer 3'-end. Thus, in primosome, p58_C works as a processivity factor for Pol α , providing quick intramolecular reloading of the template:primer to the active center of a DNA polymerase. This conclusion is supported by the fact that the DNA trap is not efficient in blocking the Pol α active site during synthesis of a 32-mer primer by primosome (Figure 2B).

The two-point interaction mode between the primer and primosome, with p58_C at the 5'-end and p180_{core} at the 3'-end, predicts an increase in the distance between these domains during primer extension and stretching of the linkers L1 and L2, which tether p58_C and p180_{core} to the platform. To test this hypothesis, we generated one Pol α mutant by

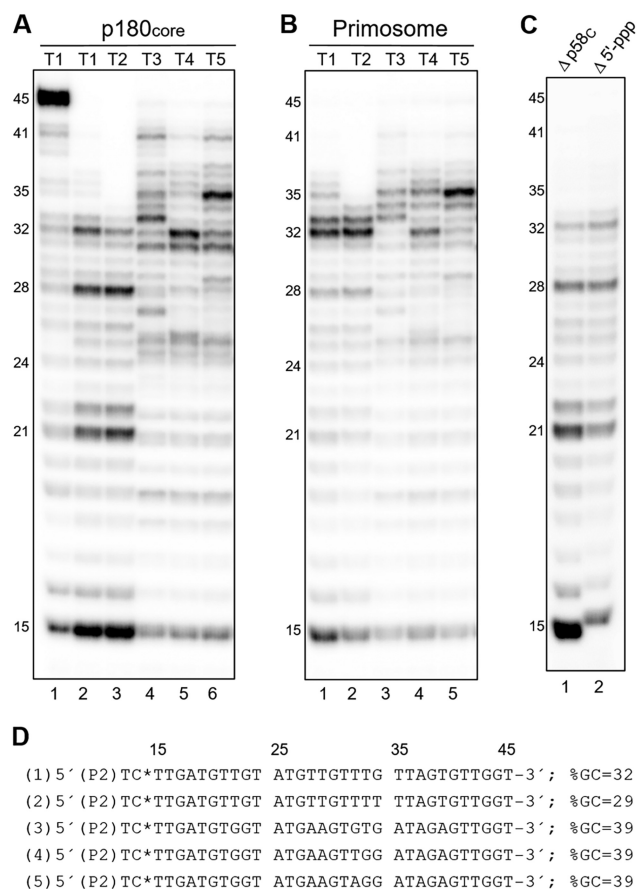


Figure 2. Analysis of DNA synthesis elongation and termination by p180_{core} and primosome. The products generated by p180_{core} and primosome on templates T1-T5 annealed to the 12-mer primer P2 are shown on panels (A) and (B), respectively. (C) Primosome shows reduced processivity of DNA synthesis when the primer-p58C interaction is disrupted. Lane 1 – T1:P2 and primosome with deleted p58C; lane 2 – T1:P1 (primer without 5'-triphosphate) and primosome. (D) Sequences of synthesized primers. The numbers of corresponding templates are shown in parenthesis. Asterisk indicates a position of [α -³²P]-label. GC content (shown as %GC) was calculated for indicated primer sequences. Reactions contained 0.6 μ M template:primer, 0.2 μ M enzyme, 10 μ M dNTPs, 0.1 μ M [α -³²P]-dCTP, and 10 μ M trap (except lane 1 on panel A), and were incubated at 35°C for 30 s. The products were resolved by 20% urea-PAGE and visualized by phosphorimaging.

deleting 8aa in L2 as well as four primase mutants by insertion of five amino acids (aa) or by deleting five, ten, and fifteen aa in L1. Eight primosome mutants, containing different combinations of linkers in primase and Pol α , were obtained (Supplemental Figure S2) and tested in a primer extension assay on T1 (Figure 3). The 5aa extension of L1 resulted in 1.9-fold increase in the level of 35- to 37-mer products versus those 32- to 33-mer in length (Figure 3A, comparison of lanes 1 and 3, and Figure 3B). L1 shortening by 5aa had a small effect on products distribution (Figure 3A, lane 5), while deletion of 10aa and especially 15aa significantly raised the level of immature primers (lanes 7–10). For example, the level of a 28-mer product increased 3.4-fold in the case of a 15aa deletion in L1 and 7-fold when this L1 truncation was combined with an 8aa deletion in L2 (Figure 3B).

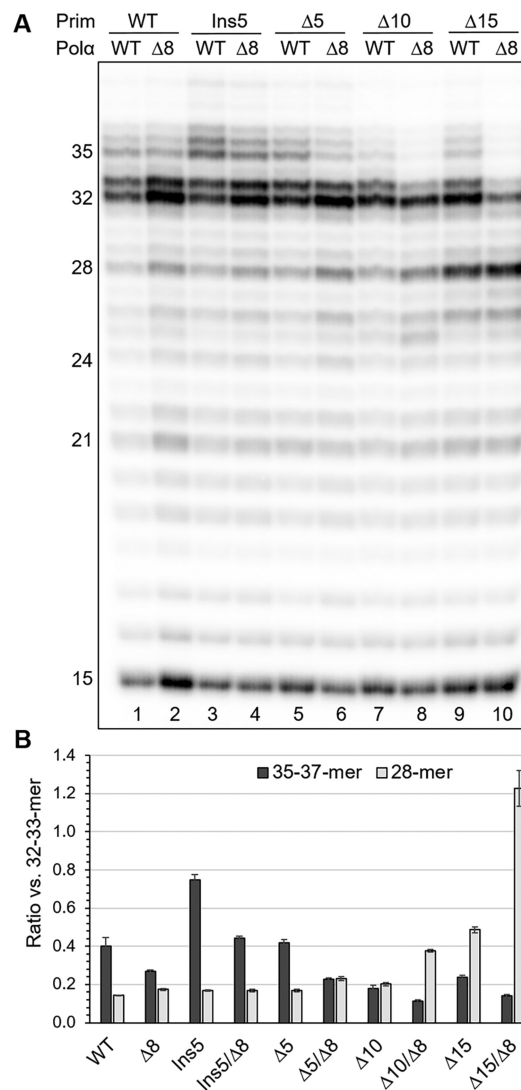


Figure 3. The linkers in primase and Pol α regulate the primer length. (A) Analysis of primer extension products generated by primosome and its mutants. Lane 1 – T1:P2 and primosome with intact linkers. Lanes 2–10 – T1:P2 and primosome mutants with linker modifications in primase and Pol α . Δ5, Δ10, Δ15 and Ins5 denotes deletion of 5aa, 10aa, 15aa and insertion of 5aa into primase linker, respectively. Δ8 denotes deletion of 8aa in Pol α linker. (B) Effect of linkers length on the level of selected products (see the panel A). The data are presented as bar graphs showing the mean \pm SD calculated from three independent experiments (Supplemental Figure S4).

Table 2. Results of binding studies

Protein	dTTP ^a	$k_{\text{off}} \times 10^{-3} \text{ s}^{-1}$	$k_{\text{on}} \text{ mM}^{-1} \text{ s}^{-1}$	K_{D}^{b} nM
p58C	-	4.0 \pm 0.12	286 \pm 31	14.0 \pm 1.6
Pol α (28)	-	340 \pm 42	242 \pm 12	1400 \pm 130
	+	43.5 \pm 5.8	259 \pm 9.9	168 \pm 17

^adTTP was added at a concentration of 50 μ M, together with 5 mM MgCl₂.

^b K_{D} values are obtained by dividing k_{off} by k_{on} . Data are presented as mean \pm SD.

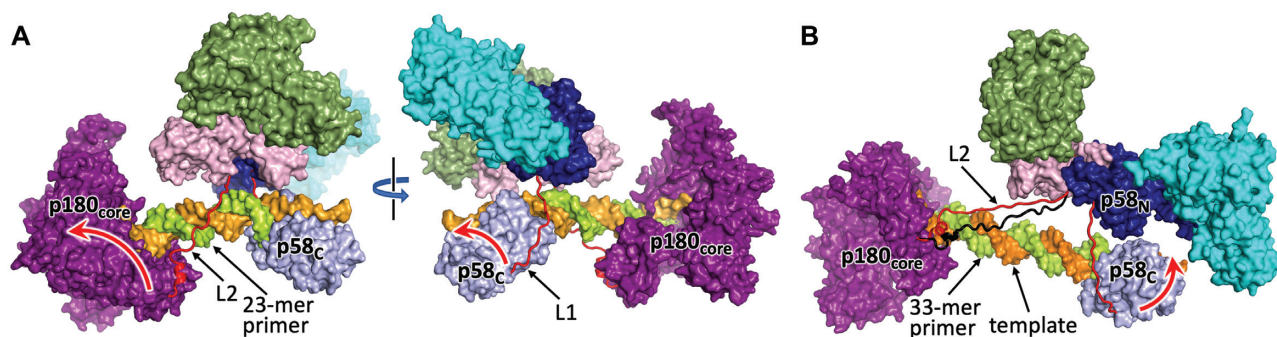


Figure 4. The structure-based models of a primosome elongation complexes. Models with 23-mer (A) and 33-mer primers (B) are shown. Coloring of domains is the same as in Figure 1. The linkers are represented as cartoons and colored red. Red arrows indicate the direction of domains movement upon primer extension. In panel (B), L2 with partially unfolded helix is colored black.

In summary, these data support the idea that the L1 and L2 linkers play a role in DNA synthesis termination by controlling the primer length. Of note, Pol α residues 1240–1249 may turn to the coil (Supplemental Figure S3) and become the part of L2 extending its length to 28aa. Moreover, there is a L3 linker in p180 (1445–1447) that tethers p180_C to p58_N and makes the platform flexible between the points of L1 and L2 attachment to it (Figure 1). These factors may help the mutated primosome to partially compensate for a reduction in linker length.

Stability of p58_C/template:primer complex defines DNA synthesis termination

We estimated stability of the p58_C complex with a T7:P2 duplex containing the 12-mer chimeric RNA–DNA primer that was used in primer extension studies (Table 1) and has a 5′-triphosphate. Binding studies were conducted on Octet K2, which allows for extracting the rate constants of complex formation (k_{on}) and dissociation (k_{off}) and calculating the dissociation constant (K_D). Recently, we applied this approach to studying the binding kinetics for Pol α and DNA (28). A 26-mer DNA template T7 with biotin at the 5′-end was primed by a 12-mer primer P2 and loaded on a streptavidin-coated sensor.

An obtained k_{off} value of 0.004 s⁻¹ points out to a stable p58_C/T7:P2 complex with a half-life of ~3 min (Table 2). In comparison, Pol α shows 11-fold and 85-fold less stable interaction with a template:primer in the presence and absence of incoming dNTP, respectively. According to these data, Pol α has a significantly higher probability than p58_C to dissociate from the mature primer when the tension in the stretched linkers is built up, resulting in DNA synthesis termination. The K_D value of 14 nM obtained here for the p58_C/T7:P2 complex (Table 2) is 2-fold lower than the value that we obtained previously by using a gel-retardation assay and a 7-mer primer (25). Taking into account the differences in employed approaches and experimental setup, we can conclude that in general these results are consistent.

To evaluate a consistency of our data with a structural potential of a primosome to stretch the linkers we obtained several structure-based models. At initial steps of dNMPs incorporation by Pol α , the length of linkers is sufficient for

free spiral rotational movement of p58_C relative to p180_{core}. However, the options for linkers become increasingly limited during the last helical turn. As illustrated in Figure 4A with a 23-mer RNA–DNA primer, both L1 and L2 linkers are in extended conformation, but still not fully stretched. Addition of a half helical turn to the template–primer duplex moves the end of L1 and the beginning of L2 closer to the platform, thus providing some relaxation for the linkers. Upon addition of more dNMPs, these ends of L1 and L2 will move away from the platform resulting in almost fully stretched linkers with 32- or 33-mer primers (Figure 4B).

DISCUSSION

Our studies unveiled the intricate mechanism of RNA–DNA primer length counting by primosome. This mechanism is based on stable p58_C interaction with a template:primer, which boosts Pol α processivity during primer maturation. The two-point binding mode of a template:primer by primosome, with p58_C at the primer 5′-end and p180_{core} at the 3′-end, dictates the involvement of primosome linkers L1 and L2 in primer length counting and DNA synthesis termination (Figure 4). These linkers, with a cumulative length of 36aa, act as springs, requiring some energy for stretching. Probably, this energy comes from hydrolysis of the phosphodiester bond of dNTPs. Upon addition of 23–28 dNMPs, the accumulated tension in the stretched linkers gradually increases probability of p180_{core} ejection from the duplex and DNA synthesis termination. Once the mature primer is dissociated from p180_{core}, reloading of p58_C-bound template:primer to the Pol α active site is complicated because it requires significant spontaneous stretching of the linkers. Thus, p58_C is a crucial element in DNA synthesis termination. Due to the mutagenic potential of Pol α (8), which does not possess proofreading exonuclease activity, limitation of a DNA track to ~25nt is important for genome stability.

The obtained data allow us to conclude that p58_C is a critical regulator of all steps of RNA–DNA primer synthesis, from RNA synthesis initiation by primase until DNA synthesis termination by Pol α . After initiation, elongation, and termination of RNA–DNA primer synthesis, p58_C may stay bound to the 5′-end of a primer and, consequently, par-

participates in primer handoff from Pol α to Pol ϵ and Pol δ , possibly by facilitating RFC/PCNA loading. Interestingly, because p58_C is also responsible for initiation of RNA primer synthesis, primosome stays autoinhibited until p58_C dissociates from the previously synthesized primer. Considering the relatively long half-life of the complex with a template:primer, p58_C may remain bound to it until completion of Okazaki fragment synthesis that only takes seconds (29,30). Thus, p58_C recycling may emerge as a key aspect of controlling events at the replication fork, both spatially and temporally. For example, p58_C may prevent PCNA from sliding off from the primer 5'-end after RFC dissociation.

SUPPLEMENTARY DATA

Supplementary Data are available at NAR Online.

ACKNOWLEDGEMENTS

We thank K. Jordan for editing this manuscript.

Author contributions: A.G.B. developed the protocol for chimeric primer synthesis, carried out the biochemical experiments, and supervised preparation of samples for functional studies. L.M.M., A.E.L. and N.D.B. participated in preparation of samples and technical support. T.H.T. initiated the project, performed modeling, and proposed and clarified the mechanism of termination with the help of team members. T.H.T. and A.G.B. wrote the manuscript.

FUNDING

National Institute of General Medical Sciences [R35GM127085 to T.H.T.]. Funding for open access charge: National Institute of General Medical Sciences [R35GM127085].

Conflict of interest statement. None declared.

REFERENCES

- Baranovskiy, A.G. and Tahirov, T.H. (2017) Elaborated action of the human primosome. *Genes (Basel)*, **8**, 62.
- Pellegrini, L. (2012) The pol alpha-primase complex. *Subcell. Biochem.*, **62**, 157–169.
- Casteel, D.E., Zhuang, S., Zeng, Y., Perrino, F.W., Boss, G.R., Goulian, M. and Pilz, R.B. (2009) A DNA polymerase- α primase cofactor with homology to replication protein A-32 regulates DNA replication in mammalian cells. *J. Biol. Chem.*, **284**, 5807–5818.
- Mizuno, T., Hirabayashi, K., Miyazawa, S., Kobayashi, Y., Shoji, K., Kobayashi, M., Hanaoka, F., Imamoto, N. and Torigoe, H. (2021) The intrinsically disordered N-terminal region of mouse DNA polymerase alpha mediates its interaction with POT1a/b at telomeres. *Genes Cells*, **26**, 360–380.
- Starokadomskyy, P., Gemelli, T., Rios, J.J., Xing, C., Wang, R.C., Li, H., Pokatayev, V., Dozmorov, I., Khan, S., Miyata, N. et al. (2016) DNA polymerase-alpha regulates the activation of type I interferons through cytosolic RNA:DNA synthesis. *Nat. Immunol.*, **17**, 495–504.
- Kilkenny, M.L., Veale, C.E., Guppy, A., Hardwick, S.W., Chirgadze, D.Y., Rzechorzek, N.J., Maman, J.D. and Pellegrini, L. (2022) Structural basis for the interaction of SARS-CoV-2 virulence factor nsP1 with DNA polymerase alpha-primase. *Protein Sci.*, **31**, 333–344.
- Tang, L., Sheraz, M., McGrane, M., Chang, J. and Guo, J.T. (2019) DNA polymerase alpha is essential for intracellular amplification of hepatitis B virus covalently closed circular DNA. *PLoS Pathog.*, **15**, e1007742.
- Reijns, M.A.M., Kemp, H., Ding, J., de Proce, S.M., Jackson, A.P. and Taylor, M.S. (2015) Lagging-strand replication shapes the mutational landscape of the genome. *Nature*, **518**, 502–506.
- Schimmel, J., Munoz-Subirana, N., Kool, H., van Schendel, R. and Tijsterman, M. (2021) Small tandem DNA duplications result from CST-guided pol alpha-primase action at DNA break termini. *Nat. Commun.*, **12**, 4843.
- Mirman, Z., Lotterberger, F., Takai, H., Kibe, T., Gong, Y., Takai, K., Bianchi, A., Zimmermann, M., Durocher, D. and de Lange, T. (2018) 53BP1-RIF1-shieldin counteracts DSB resection through CST- and Polalpha-dependent fill-in. *Nature*, **560**, 112–116.
- Han, T., Goralski, M., Capota, E., Padrick, S.B., Kim, J., Xie, Y. and Nijhawan, D. (2016) The antitumor toxin CD437 is a direct inhibitor of DNA polymerase alpha. *Nat. Chem. Biol.*, **12**, 511–515.
- Burgers, P.M.J. and Kunkel, T.A. (2017) Eukaryotic DNA replication fork. *Annu. Rev. Biochem.*, **86**, 417–438.
- Pellegrini, L. and Costa, A. (2016) New insights into the mechanism of DNA duplication by the eukaryotic replisome. *Trends Biochem. Sci.*, **41**, 859–871.
- Baranovskiy, A.G., Zhang, Y., Suwa, Y., Babayeva, N.D., Gu, J., Pavlov, Y.I. and Tahirov, T.H. (2015) Crystal structure of the human primase. *J. Biol. Chem.*, **290**, 5635–5646.
- Baranovskiy, A.G., Babayeva, N.D., Zhang, Y., Gu, J., Suwa, Y., Pavlov, Y.I. and Tahirov, T.H. (2016) Mechanism of concerted RNA-DNA primer synthesis by the human primosome. *J. Biol. Chem.*, **291**, 10006–10020.
- Nunez-Ramirez, R., Klinge, S., Sauguet, L., Melero, R., Recuero-Checa, M.A., Kilkenny, M., Perera, R.L., Garcia-Alvarez, B., Hall, R.J., Nogales, E. et al. (2011) Flexible tethering of primase and DNA pol alpha in the eukaryotic primosome. *Nucleic Acids Res.*, **39**, 8187–8199.
- Sheaff, R.J. and Kuchta, R.D. (1993) Mechanism of calf thymus DNA primase: slow initiation, rapid polymerization, and intelligent termination. *Biochemistry*, **32**, 3027–3037.
- Copeland, W.C. and Wang, T.S. (1993) Enzymatic characterization of the individual mammalian primase subunits reveals a biphasic mechanism for initiation of DNA replication. *J. Biol. Chem.*, **268**, 26179–26189.
- Kuchta, R.D., Reid, B. and Chang, L.M. (1990) DNA primase. Processivity and the primase to polymerase alpha activity switch. *J. Biol. Chem.*, **265**, 16158–16165.
- Sheaff, R.J., Kuchta, R.D. and Ilseley, D. (1994) Calf thymus DNA polymerase alpha-primase: “communication” and primer-template movement between the two active sites. *Biochemistry*, **33**, 2247–2254.
- Murakami, Y., Eki, T. and Hurwitz, J. (1992) Studies on the initiation of simian virus 40 replication in vitro: RNA primer synthesis and its elongation. *Proc. Natl. Acad. Sci. U.S.A.*, **89**, 952–956.
- Baranovskiy, A.G., Gu, J., Babayeva, N.D., Agarkar, V.B., Suwa, Y. and Tahirov, T.H. (2014) Crystallization and preliminary X-ray diffraction analysis of human DNA primase. *Acta Crystallogr. F Struct. Biol. Commun.*, **70**, 206–210.
- Zhang, Y., Baranovskiy, A.G., Tahirov, T.H. and Pavlov, Y.I. (2014) The C-terminal domain of the DNA polymerase catalytic subunit regulates the primase and polymerase activities of the human DNA polymerase alpha-primase complex. *J. Biol. Chem.*, **289**, 22021–22034.
- Liu, H. and Naismith, J.H. (2008) An efficient one-step site-directed deletion, insertion, single and multiple-site plasmid mutagenesis protocol. *BMC Biotechnol.*, **8**, 91.
- Baranovskiy, A.G., Zhang, Y., Suwa, Y., Gu, J., Babayeva, N.D., Pavlov, Y.I. and Tahirov, T.H. (2016) Insight into the human DNA primase interaction with template-primer. *J. Biol. Chem.*, **291**, 4793–4802.
- Baranovskiy, A.G., Duong, V.N., Babayeva, N.D., Zhang, Y., Pavlov, Y.I., Anderson, K.S. and Tahirov, T.H. (2018) Activity and fidelity of human DNA polymerase alpha depend on primer structure. *J. Biol. Chem.*, **293**, 6824–6843.

27. Emsley, P., Lohkamp, B., Scott, W.G. and Cowtan, K. (2010) Features and development of coot. *Acta. Crystallogr. D Biol. Crystallogr.*, **66**, 486–501.
28. Baranovskiy, A.G., Babayeva, N.D., Lisova, A.E., Morstadt, L.M. and Tahirov, T.H. (2022) Structural and functional insight into mismatch extension by human DNA polymerase α . *Proc. Natl. Acad. Sci. U.S.A.*, **119**, e2111744119.
29. Raghuraman, M.K., Winzeler, E.A., Collingwood, D., Hunt, S., Wodicka, L., Conway, A., Lockhart, D.J., Davis, R.W., Brewer, B.J. and Fangman, W.L. (2001) Replication dynamics of the yeast genome. *Science*, **294**, 115–121.
30. Stodola, J.L. and Burgers, P.M. (2016) Resolving individual steps of Okazaki-fragment maturation at a millisecond timescale. *Nat. Struct. Mol. Biol.*, **23**, 402–408.